Effect of ZnO on the microstructure and electrical properties of WO_3-$Bi_4Ti_3O_{12}$ ceramics

M. Villegas[1], T. Jardiel, A.C. Caballero

Dept. Electroceramics. Instituto de Cerámica y Vidrio – CSIC.

28049 Cantoblanco. Madrid. Spain

ABSTRACT

The aim of the present work is to explore the possibility of incorporate a small amount of ZnO to improve the microstructure control of W-doped BIT based materials. Two different processing routes have been used according to previous results reported for other materials: reaction and sintering in one single step and a previous calcination step. The sintering behaviour of the samples, the obtained crystalline phases and the microstructure analysis indicate that the reaction between ZnO and Bi_2O_3 plays a critical role during sintering. Both $Bi_2Ti_2O_7$ and Zn_2TiO_4 secondary phases are stabilised when adding ZnO. Actually, when WO_3 and ZnO are incorporated simultaneously to BIT materials, they interact stabilizing the $Bi_2Ti_2O_7$ phase and avoiding the incorporation of W^{6+} into the BIT lattice. As a consequence, the electrical conductivity of the samples with ZnO is two orders of magnitude higher than that of the samples doped only with WO_3, suggesting that WO_3 does not form a solid solution with BIT. The curve dielectric constant vs temperature also reveals the role played by the $Bi_2Ti_2O_7$ phase.

Keywords: Titanates, Dielectric Properties, Electrical Conductivity

---

[1] Corresponding autor. Tel.: +34 91 735 58 40; Fax: +34 91 735 58 43: e-mail: mvillegas@icv.csic.es

1

1. INTRODUCTION

$Bi_4Ti_3O_{12}$ (BIT) is a well known ferroelectric compound belonging to the Aurivillius family.[1] Due to its high Curie temperature (675ºC) it is a promising candidate for high temperature piezoelectric ceramics.[2] However its crystal symmetry[1], comprised og pseudo-perovskite units $(Bi_2Ti_3O_{10})^{2-}$ interleaved between bismuth oxide-based layers $(Bi_2O_2)^{2+}$, leads to a highly anisotropic crystal growth habit and hence to anisotropic electrical properties. The microstructure of BIT materials exhibits plate-like grains with the basal planes being parallel to the crystalline ab plane. This direction shows the maximum of the polarization and a relatively high electrical conductivity. [3,4] In fact, an increased electrical conductivity is strongly related to the presence of long platelets. An exponential dependence of the electrical conductivity with the aspect ratio (length over thickness) of the plate-like grains has been reported.[5] Therefore long plate-like grains lead to an unacceptable high electrical conductivity that hinders the poling process needed to obtain piezoelectric response in bulk ceramic materials. Since the conductivity of BIT is p-type, many efforts have been devoted to control this undesirable high electrical conductivity by both donor doping.[6,7] and by decreasing the grain size.[5]

However, controlling the anisotropic grain growth of the platelets is the main problem in the processing of BIT ceramics.[5] In addition to donor doping, the inhibition of grain growth can be obtained by different processing approaches like chemical synthesis[8,9] or particle surface modification.[10] Doping with WO_3 has proved to decrease the electrical conductivity by two orders of magnitude and this can be done for sintering temperatures around 1000 ºC.[11] However, further decrease of the electrical conductivity is needed to successfully pole BIT ceramics. Even for these W-doped materials there is a lack of reliability in the poling process and in the piezoelectric response.

For BaTiO$_3$ based materials and other perovskite based materials, doping with ZnO has been successfully applied in both controlling the grain growth and decreasing the electrical conductivity.[12] In these materials, Zn^{2+} ions segregate to the grain boundaries with two main consequences: the control of grain growth by a solute drag mechanism and the increase of the grain boundary electrical resistivity. These effects find its origin in the very low solid solubility of ZnO in the BaTiO$_3$ perovskite lattice.[13] Taking into account these results, doping with ZnO might be an interesting approach to control both the grain growth and the electrical conductivity of BIT based materials. The perovskite units of the BIT structure could be blocked by the presence of ZnO and subsequently and additional mechanism for grain growth control could be activated for W-doped BIT materials.

The aim of the present work is to explore the possibility of incorporate a small amount of ZnO to improve the microstructure control of W-doped BIT based materials. For this purpose different processing routes have been used according to previous results reported for other materials. The microstructure evolution as well as the influence of ZnO on both the dielectric constant and the electrical conductivity is also addressed.

2. EXPERIMENTAL PROCEDURE

Samples were prepared from high purity (99.99%) oxide precursors. TiO$_2$, Bi$_2$O$_3$, WO$_3$ and ZnO were used as starting materials for the preparation of Bi$_4$Ti$_3$W$_{0.05}$O$_{12.15}$ (WBIT) ceramics and with 2 and 5 wt% additions of ZnO (WBIT-2Zn and WBIT-5Zn respectively). The appropriate amounts of the starting oxides were mixed in an attrition mill with ZrO$_2$ balls and ethanol as mixing media. After drying and sieving the powder, two different processing approaches were carried out. In one case, samples were pressed into disks of 15 mm diameter and 1.5mm thickness and reaction-sintered at 1000ºC for 2 hours. In the second approach the powder was treated at 800ºC for 2 hours; then it was attrition milled, and disks were pressed and sintered at the same temperature (1000 ºC for 2 hours).Reaction-sintered ceramics will be hereafter

designated as RS and the calcined ones as C. In order to clarify some results, $Bi_2Ti_2O_7$ ceramics with 5%wt ZnO were prepared in the same conditions as the C samples. The sintering behaviour was measured by a horizontal-loading dilatometer (DI-24 Adamel-L'homargi) from 25º to 1150ºC, using a heating rate of 3ºC/min. The crystalline phases present in the samples were characterized by X-Ray Diffraction (XRD, Siemens D5000, CuK$_\alpha$ radiation) and the microstructure was observed on polished and thermally etched surfaces by Field-Emission Scanning Electron Microscopy (FE-SEM, Hitachi S4700) equipped with EDS. The dielectric constant and the electrical conductivity were determined in the 25º-740ºC temperature range by means of an impedance analyzer Agilent 4294A on samples electroded with Ag paste.

3- RESULTS AND DISCUSSION

3.1 Sintering behaviour

Shrinkage curves obtained from constant heating rate experiments are shown in figure1. The samples WBIT_RS and WBIT-2Zn_RS (reacted and sintered in a single step) show a slight expansion which corresponds to the formation of $Bi_4Ti_3O_{12}$.[14,15]. However for the WBIT-2Zn_RS sample, the expansion is observed at higher temperature (around 50ºC) and is markedly lower than that for sample WBIT_RS. This points out that a shrinkage mechanism is overlapped to the expansion related to the BIT formation. In fact at temperatures within the 740-750ºC range it is reported the appearance of a liquid phase according to the ZnO-Bi_2O_3 phase equilibrium diagram[16]. Therefore it is reasonable to presume that the reaction between ZnO and Bi_2O_3 to form a Bi-rich liquid phase containing ZnO retards the beginning of the BIT formation and leads to an early shrinkage mechanism.

For the previously calcined ZnO doped samples (C samples) the beginning of shrinkage decreases around 200ºC compared to pure WBIT. Since the temperature of the liquid formation is the same for all the doped samples (740-750 ºC), shrinkage will also start at the same temperature for WBIT-2Zn_RS and therefore the differences in

the expansion for the WBIT_RS and WBIT-2Zn_RS samples can be completely explained. In view of these results it seems that the reaction between ZnO and Bi_2O_3 plays a dominant role in both processing routes. Such reaction leads to a low temperature liquid phase by either the formation of the sillenite phase $19Bi_2O_3 \cdot ZnO$ which melts around 750ºC[16] or the appearance of liquid at 743ºC because of the eutectic point. ZnO containing samples show a second shrinkage change at temperatures above 1050º which is caused by the presence of a large amount of liquid phase. After these experiments samples were deformed and showed glassy surfaces. Taking into account the constant heating rate experiments, pressed disks of the different materials were sintered at 1000ºC for two hours. Except for the case of the WBIT-5Zn_RS, the sintered pellets exhibit densities higher than 96% of the BIT theoretical density. Samples doped with 5 w% of ZnO and reaction-sintered at different temperatures showed extensive cracking and/or high porosity.

3.2 XRD Characterization

XRD patterns of calcined powders (WBIT_C and WBIT-5Zn_C) are shown in Figure 2.a. For pure WBIT only the $Bi_4Ti_3O_{12}$ phase was detected, however WBIT-5Zn is a mixture of $Bi_4Ti_3O_{12}$ and $Bi_2Ti_2O_7$. The analysis of the sintered samples (Figure 2.b) revealed that WBIT_RS, WBIT_C and WBIT-2Zn_C samples only showed $Bi_4Ti_3O_{12}$. Meanwhile WBIT-2Zn_RS sample seems to show small traces of $Bi_2Ti_2O_7$, and its presence was confirmed by SEM analysis (later on the text). The amount of this phase increased with ZnO and additionally some traces of Zn_2TiO_4 spinel can be detected for the WBIT-5Zn_C sample[17]. The XRD pattern of WBIT-5Zn_C sample showed a higher orientation of the platelets in the (0k0) direction which can be caused by the high length of the plate-like grains. $Bi_2Ti_2O_7$ is a $A_2B_2O_7$ compound with pyrochlore structure which is stable at low temperature (700ºC) and when heated transforms into $Bi_4Ti_3O_{12}$ and $Bi_2Ti_4O_{11}$.[18] However $Bi_2Ti_2O_7$ can be stabilized by doping.[19] In this case, it is clear that

the addition of ZnO stabilizes the $Bi_2Ti_2O_7$ phase and consequently materials with two or three phases are obtained.

3.3 Microstructure Characterization

Figure 3 shows the microstructure of WBIT samples sintered at 1000ºC/2h. Different microstructures are observed when comparing WBIT_C and WBIT_RS samples. As expected, the C sample shows a homogeneous single phase microstructure with plate-like grains of W-doped $Bi_4Ti_3O_{12}$ about 2-3µm in length. On the contrary, for the reaction sintered sample, some grains of a secondary phase which was not detected by XRD could be observed along with $Bi_4Ti_3O_{12}$ plate-like grains (Figure 3.b). EDS analysis of this phase revealed that its composition is close to that of $Bi_2Ti_2O_7$. In this case, the presence of W(VI) seems to stabilize the $Bi_2Ti_2O_7$ phase at temperatures higher than 700ºC and retards the formation of $Bi_4Ti_3O_{12}$. For the WBIT_C sample, when the powder is calcined, the subsequent milling step re-activates the particles and the formation of $Bi_4Ti_3O_{12}$ can be completed.

Figure 4 shows the microstructure of ZnO-doped samples. As it was mentioned above in the XRD characterization, the WBIT-2Zn_RS samples show the presence of some areas with relatively small faceted grains whose composition analysed by EDS is again very close to of the $Bi_2Ti_2O_7$ phase (figure 4a). No phases with ZnO were detected neither by XRD or SEM. This might be caused by a very low concentration but it is also possible that the Zn^{2+} might be incorporated into the $Bi_4Ti_3O_{12}$ or $Bi_2Ti_2O_7$ lattices. Also these samples show a dual platelet size which is usual in BIT based ceramics; platelets of about 5µm coexist with much bigger platelets (fig 4.b). For the WBIT-2Zn_C samples (figure 4c) no significant differences compared to the reaction-sintered compositions are observed. In the case of the WBIT-5Zn_C samples, platelets with $Bi_4Ti_3O_{12}$ composition along with some dark grains and some faceted grains are observed (Figure 4.d). EDS analysis of these dark grains revealed that the Zn/Ti ratio is 2.1, close to that of Zn_2TiO_4 spinel phase. This result was expected since traces of this

phase were also observed by XRD. On the other hand, the faceted grains observed in the microstructure seem to correspond to the $Bi_2Ti_2O_7$ phase as for the 2w% ZnO-doped samples.


3.4 Electrical Characterization

Figure 5 shows the dependence of the dielectric constant with the temperature (at 1 MHz) for different samples. Two different features can be clearly observed related to the ZnO incorporation: the presence of a double peak and the increase of the transition temperature. The change of the curve shape after T_c for the WBIT-2Zn_RS sample becomes a clear shoulder for the sample WBIT-5Zn_C. In this last case the two transitions take place at 670ºC and 695ºC, being the first the Curie temperature of $Bi_4Ti_3O_{12}$ and the second the Curie temperature of $Bi_2Ti_2O_7$.[20] This dielectric behaviour coincides with the secondary phases observed in the microstructure and in the XRD patterns. The Curie temperature of WBIT is about 15ºC lower than that of ZnO doped WBIT ceramics and corresponds to the Tc of WO_3-doped BIT[21] ceramics. This behaviour points out that in the samples with ZnO additions the WO_3 does not enter into the BIT lattice to form solid solution.

Figure 6 shows the Arrhenius plots of the electrical conductivity in the ferroelectric phase (T≤600ºC) for the different samples. As it can be seen, WBIT-2Zn and WBIT-5Zn ceramics exhibit a relatively high conductivity, very similar to the conductivity values of undoped BIT[22]. On the other hand the ceramics with no ZnO added show an electrical conductivity which is about two orders of magnitude lower, as expected for WO_3-doped BIT[5]. The fact that the slope of the conductivity does not change indicates that the conduction mechanism is also the same and probably only the charge carrier concentration is responsible for this increase in the conductivity. Taking into account these results and the microstructure analysis, the increase of the conductivity in ZnO-WO_3 co-doped BIT ceramics occurs because WO_3 is trapped in the secondary phases and does not form a BIT solid solution. This behaviour seems to be originated in the

7

stabilisation of the $Bi_2Ti_2O_7$ phase which is the point in common for WBIT-2Zn and WBIT-5Zn samples.

3.5 Influence of $Bi_2Ti_2O_7$ secondary phase on the electrical properties of BIT-based ceramics

At this point it is necessary to clarify if the presence of the $Bi_2Ti_2O_7$ secondary phase is responsible for the observed behaviour of both the dielectric constant and the electrical conductivity of these materials. For this purpose 5wt% ZnO-doped $Bi_2Ti_2O_7$ ceramics were prepared. Samples of previously calcined powders (as C samples) were pressed and sintered at 1000ºC. High density (>98% theoretical density) materials were obtained. The XRD characterization (figure 7) showed a mixture of $Bi_2Ti_2O_7$, $Bi_4Ti_3O_{12}$ and traces of Zn_2TiO_4 spinel. The following reactions could be considered to describe the reaction path:

$$Bi_2O_3 + 2TiO_2 \xrightarrow{\text{ZnO}} Bi_2Ti_2O_7$$

$$2\,Bi_2Ti_2O_7 \xrightarrow{\text{ZnO}} Bi_4Ti_3O_{12} + Zn_2TiO_4$$
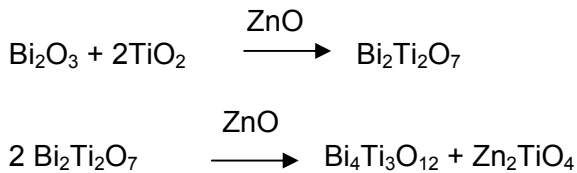
The microstructure of $Bi_2Ti_2O_7$ (figure 8) confirmed the presence of the crystalline phases observed by XRD, being a mixture of BIT, $Bi_2Ti_2O_7$ and Zn_2TiO_4.

At this point, a question raises about the presence of W(VI). By means of EDS measurements a small signal of W is detected in areas where fine rounded grains are observed, i.e., areas with a mixture of the Zn_2TiO_4 and $Bi_2Ti_2O_7$ phases. However, if large $Bi_4Ti_3O_{12}$ grains are analyzed no W signal is observed. These results indicate again that W^{6+} does not enter into the BIT lattice.

When representing the dielectric constant as a function of temperature (figure 9.a) a very low dielectric constant is obtained compared with that of BIT. The double peak present in the ZnO-doped WBIT ceramics is also observed. Therefore it can be stated that this double T_c peak and the low dielectric constant are due to the presence of the

secondary $Bi_2Ti_2O_7$ phase. The Arrhenius plots of the electrical conductivity (figure 9.b) shows that the values of the ZnO-doped $Bi_2Ti_2O_7$ ceramics are approximately one order of magnitude lower than those of ZnO-doped WBIT ceramics, but one order of magnitude higher than those of WBIT. It can be thus concluded that when WO_3 and ZnO are used simultaneously, they interact to stabilize the $Bi_2Ti_2O_7$ phase and avoid the incorporation of W^{6+} into the BIT lattice.

CONCLUSIONS

BIT-based ceramics with WO_3 and ZnO additions have been prepared by two different processing approaches: reaction-sintering in a single step and a calcination step before sintering. Regardless of the processing approach, the reaction between ZnO and Bi_2O_3 plays a dominant role during sintering. A low temperature liquid phase is obtained either at the ZnO-Bi_2O_3 eutectic point (743ºC) or through the formation of the $19Bi_2O_3·ZnO$ sillenite phase that melts at 750ºC. On the other hand the interaction between WO_3 and ZnO stabilizes the $Bi_2Ti_2O_7$ phase, and also the Zn_2TiO_4 phase in the case of 5wt% ZnO-doped materials. As a consequence the incorporation of W^{6+} into the BIT lattice to form solid solution is avoided. The electrical conductivity of the samples with ZnO additions results similar to that of undoped BIT confirming that no effective WO_3 doping of the BIT phase is obtained. The dielectric constant vs temperature curve showed a double peak corresponding to the BIT and $Bi_2Ti_2O_7$ ferroelectric to paraelectric transitions.

REFERENCES

1. Aurivillius, B., Mixed Bismuth Oxides with Layer Lattices. II. Structure of $Bi_4Ti_3O_{12}$. Ark. Kemi., 1949, 1, 499-512.

2. Cummings, S.E. & Cross, L.E., Electrical and Optical Properties of Ferroelectric BIT Single Crystals. J. Appl. Phys., 1968, 39[5], 2268.

3. Subbarao, E.C., Ferroelectricity in BIT and its Solid Solutions. Phys. Rev., 1961, 122[3], 804.

4. Fouskova, A. & Cross, L.E., Dielectric Properties of Bismuth Titanate. J. Appl. Phys., 1970, 41[7], 2834-2838.

5. Villegas, M., Caballero, A.C., Moure, C., Durán, P. & Fernández, J.F., Factors Affecting the Electrical Conductivity of Donor-doped $Bi_4Ti_3O_{12}$ Piezoelectric Ceramics. J. Am. Ceram. Soc., 1999, 82[9], 2411-2419.

6. Shulman, H.S., Damjanovic, D. & Setter, N., Niobium Doping and Dielectric Anomalies in Bismuth Titanate. J. Am. Ceram. Soc., 2000, 83[3], 528-532.

7. Takahashi, M., Noguchi, Y. & Miyayama, M., Estimation of Ionic and Hole Conductivity in Bismuth Titanate Polycrystals at High Temperatures. Solid State Ionics, 2004, 172, 325-329.

8. Villegas, M., Moure, C., Fernández, J.F. & Durán, P., Preparation and Sintering Behaviour of Submicronic $Bi_4Ti_3O_{12}$ Powders, J. Mat. Sci., 1996, 31, 949-955.

9. Durán, P., Moure, C., Villegas, M., Tartaj, J., Caballero, A.C. & Fernández, J.F., Low-Temperature Synthesis of Bismuth Titanate Niobate ($Bi_7Ti_4NbO_{21}$) Nanoparticles from a Metal-Organic Polymeric Precursor. J. Am. Ceram. Soc., 2000, 83[5], 1029-1032.

10. Jardiel, T., de la Rubia, M.A. & Peiteado, M. Control of Functional Microstructure in WO_3-doped $Bi_4Ti_3O_{12}$ Ceramics. J. Am. Ceram. Soc. 2008, 91[4], 1083-1087.

11. Villegas, M., Fernández, J.F., Caballero, A.C., Modulation of Electrical Conductivity through Microstructural Control in $Bi_4Ti_3O_{12}$-based Piezoelectric Ceramics. Ferroelectrics 2002, 267, 165-173.

12. Caballero, A.C., Fernández, J.F., Moure, C., Durán, P. & Chiang, Y.M. Grain Growth Control and Dopant Distribution in ZnO-doped $BaTiO_3$. J. Am. Ceram. Soc., 1998, 81[4], 939-944.

13. Caballero, A.C., Fernández, J.F., Moure, C., Durán, P. & Fierro, J.L.G. Dopant Distribution and Grain Growth Control in $BaTiO_3$ Ceramics doped with ZnO-SiO_2-P_2O_5. J. Eur. Ceram. Soc., 1997, 17[10], 1223-1230.

14. Jovalekic, C., Aranasoska, L., Petrovic, V., & Ristic, M.M., Sintering and Characterization of $Bi_4Ti_3O_{12}$ ceramics J. Mater. Sci., 1991, 26, 3553-3564.

15. Axelsson, A.K. & Alford, N.Mc., Bismuth Titanates Candidates for High Permittivity LTCC. J. Eur. Ceram. Soc., 2006, 26, 1933-1936.

16. Serena, S., de la Rubia, M.A., Caballero, A.C. & Caballero, A. Thermodynamic Study of the Rich Bi_2O_3 Region in the Bi_2O_3-ZnO System. Bol. Soc. Esp. Ceram. V., 2006, 45[3], 150-153.

17. Manik, S.K., Bose, P. & Pradhan, S.K., Microstructure Characterization and Phase Transformation Kinetics of Ball-Milled Prepared Nanocrystalline Zn_2TiO_4 by Rietveld Method. Mater. Chem. Phys., 2003, 82, 837-847.

18. Su, W.F. & Lu, Y.T., Synthesis, Phase Transformation and Dielectric Properties of Sol-Gel Derived $Bi_2Ti_2O_7$-Ceramics. Mater. Chem. Phys., 2003, 80, 632-637.

19. Jiang, A.Q., Hu, Z.X. & Hang, L.D., The Induced Phase Transformation and Oxygen Vacancy Relaxation in La-Modified Bismuth Titanate Ceramics. Appl. Phys. Lett., 1999, 74[1], 114-116.

20. Wang, Z., Yang, C.H., Sun, D.L., Hu, J.F., Wang, H., Chen, H.C. & Fang, C.S., Atomic Force Microscopy Imaging and Wet Etching of $Bi_2Ti_2O_7$ Thin Films. Mater. Sci. Eng., 2003, B102, 335-338.

21. Lopatin, S.S., Lupeiko, T.G., Vasiltsova, T.L., Basenko, N.I. & Berlizev, I.M., Properties of Bismuth Titanate Ceramics Modified with Group V and VI elements. Inorg. Mater., 1988, 24, 1328-1331. (English Translation).

22. Azurmendi, N., Caro, I., Caballero, A.C., Jardiel T. & Villegas, M., Microwave-Assisted Reaction Sintering of Bismuth Titanate-Based Ceramics. J. Am. Ceram. Soc., 2006, 89[4], 1232-1236.

FIGURE CAPTIONS

Figure 1. Constant heating rate curves of WO_3-BIT samples with different amounts of ZnO.

Figure 2. XRD diagrams of (a) calcined samples and (b) reaction-sintered samples and calcined samples sintered at 1000ºC for 2h

Figure 3. Microstructure of polished and thermally etched surfaces of (a) WBIT_C sintered at 1000ºC/2h and (b) WBIT_RS sintered at 1000ºC/2h

Figure 4. Microstructure of polished and thermally etched surfaces of: (a) (b) WBIT-2Zn_RS sintered at 1000ºC/2h; (c) WBIT-2Zn_C sintered at 1000ºC/2h; (d) WBIT-5Zn_RS sintered at 1000ºC/2h.

Figure 5. Dielectric constant vs temperature curves for some selected samples.

Figure 6. Arrhenius plots of the electrical conductivity vs the inverse of the temperature for different samples.

Figure 7. XRD diagram of powdered sample of 5wt% ZnO-$Bi_2Ti_2O_7$ sintered at 1000ºC for 2h.

Figure 8. Microstructure of polished and thermally etched surfaces of the 5wt% ZnO-$Bi_2Ti_2O_7$ sample sintered at 1000ºC for 2h.

Figure 9. (a) Dielectric constant vs temperature curves and (b) Arrhenius plots of the electrical conductivity as a function of the inverse of the temperature for a 5wt% ZnO-$Bi_2Ti_2O_7$ sample sintered at 1000ºC for 2h.
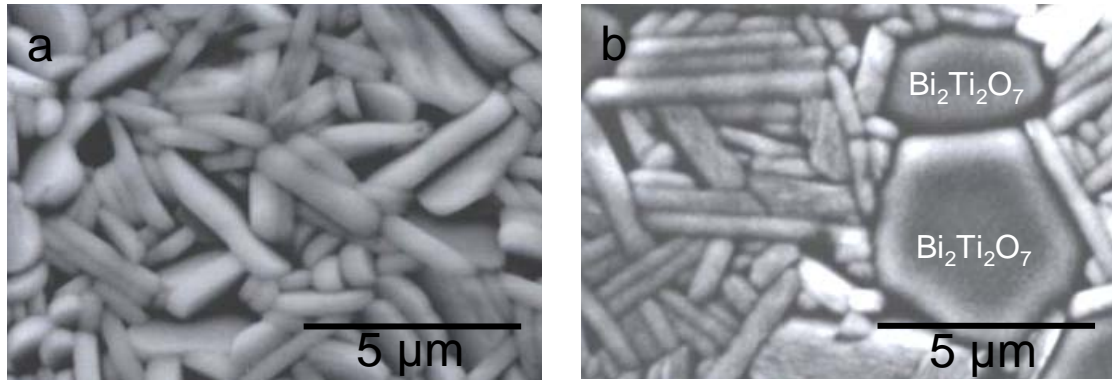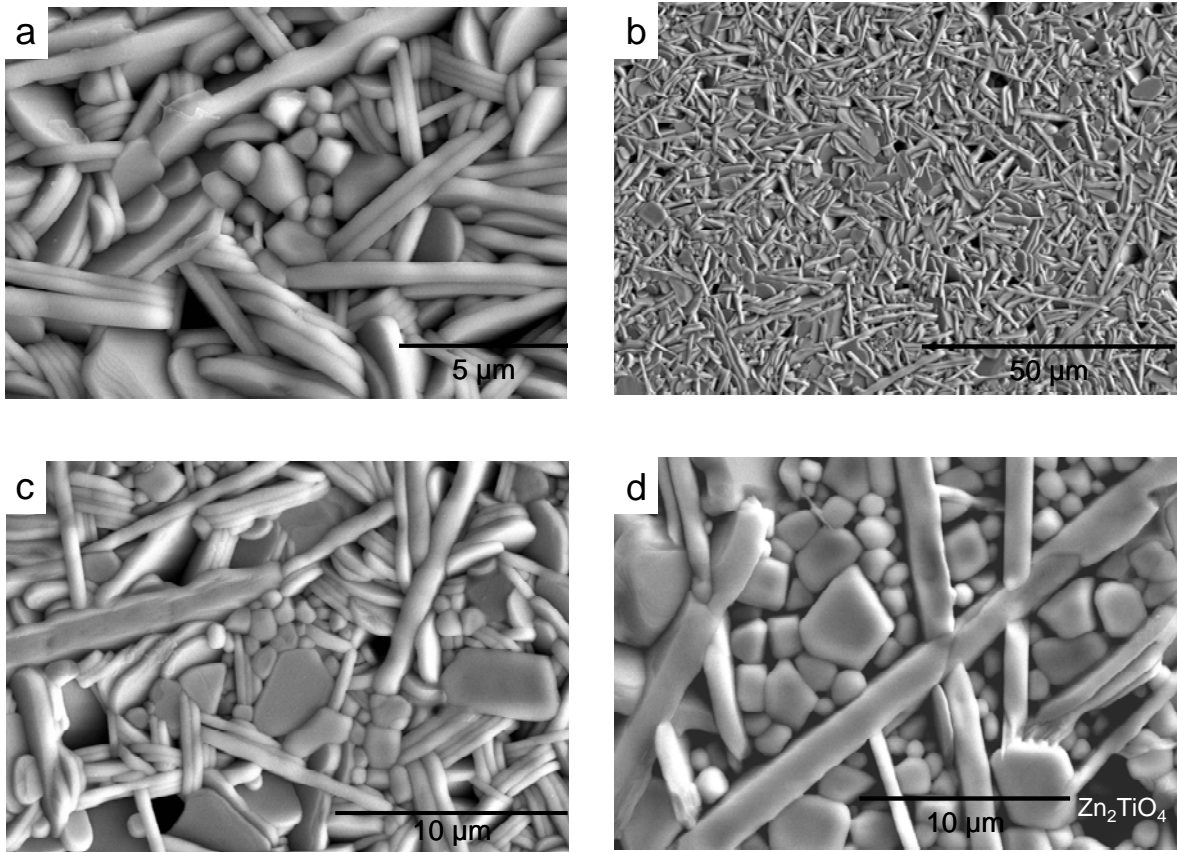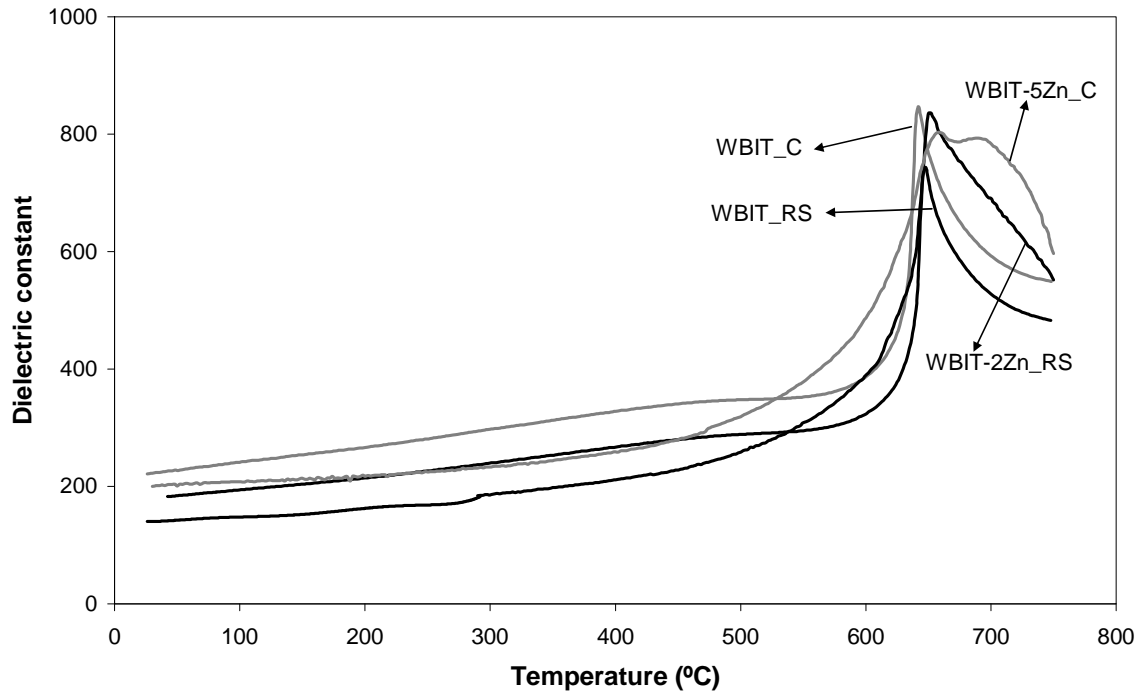
Figure 1.

M. Villegas, T. Jardiel, A.C. Caballero.

Effects of ZnO on the microstructure and electrical properties of WO_3-doped
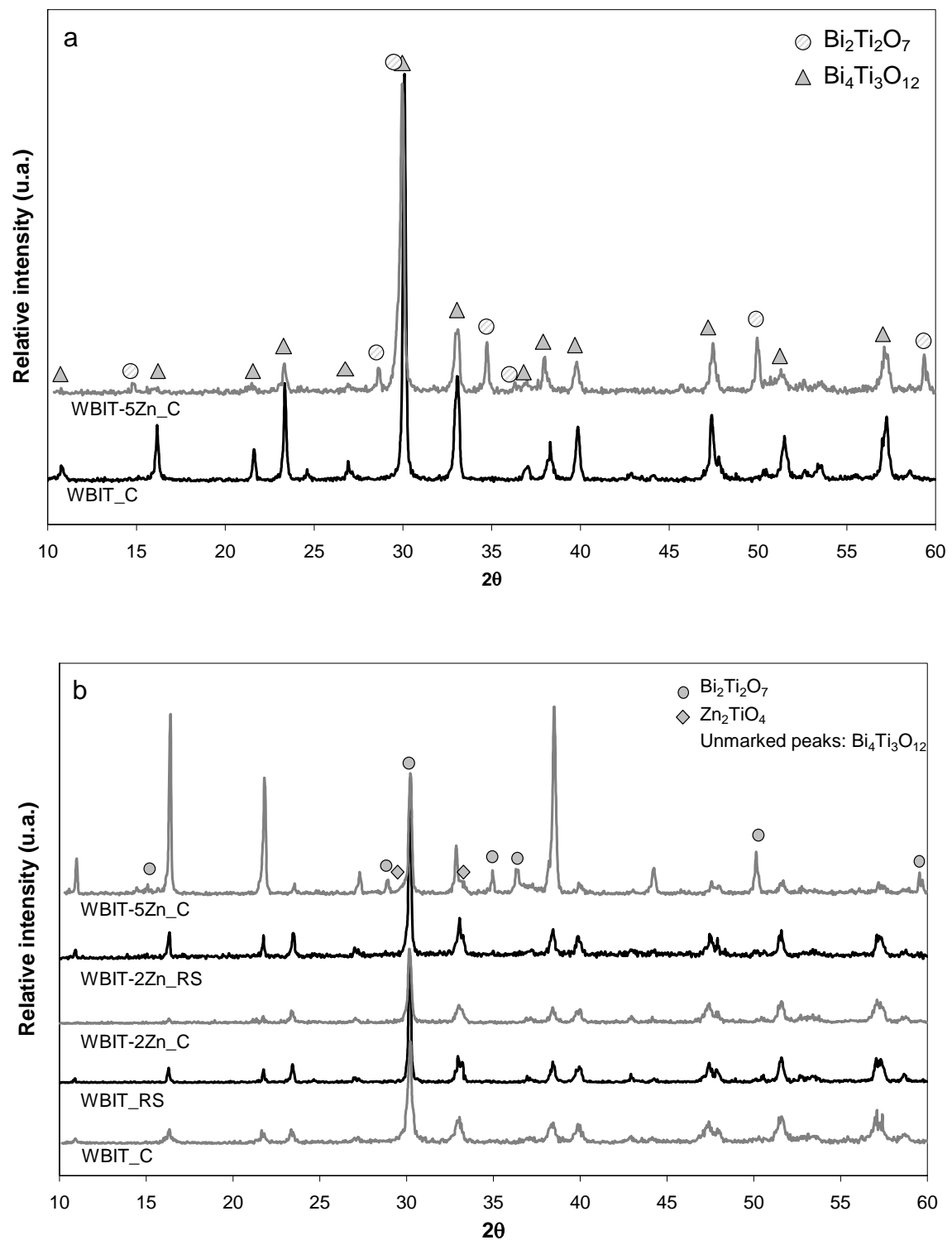
$Bi_4Ti_3WO_{12}$

Figure 2.

M. Villegas, T. Jardiel, A.C. Caballero.

Effects of ZnO on the microstructure and electrical properties of WO_3-doped
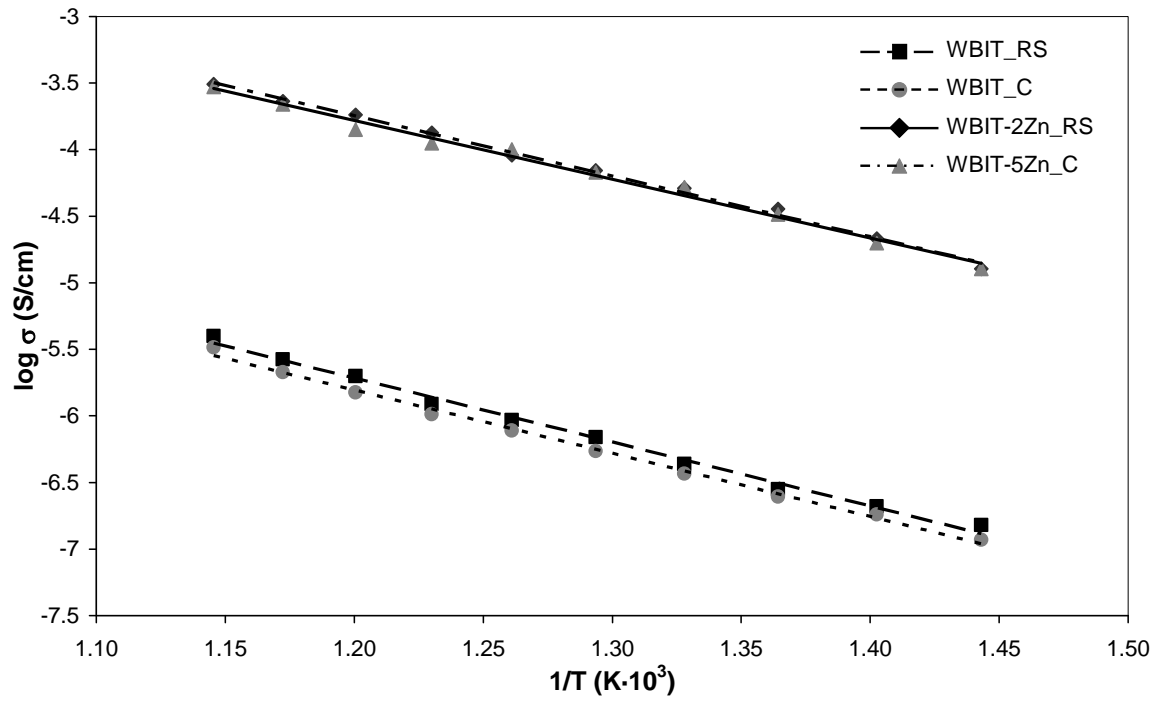
$Bi_4Ti_3WO_{12}$

Figure 3.

M. Villegas, T. Jardiel, A.C. Caballero.

Effects of ZnO on the microstructure and electrical properties of WO_3-doped

$Bi_4Ti_3WO_{12}$

Figure 4.

M. Villegas, T. Jardiel, A.C. Caballero.

Effects of ZnO on the microstructure and electrical properties of WO$_3$-doped

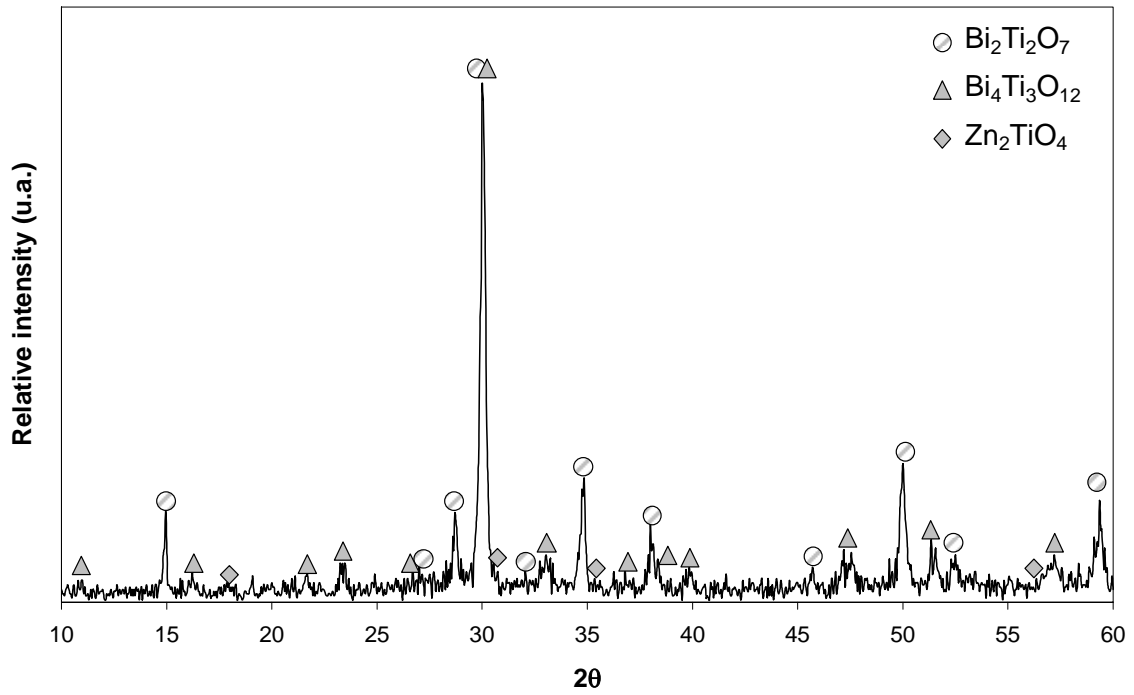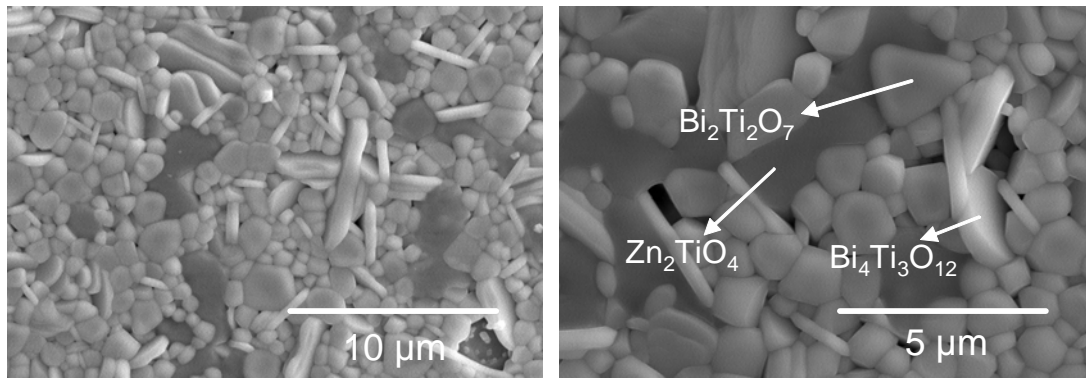Bi$_4$Ti$_3$WO$_{12}$

Figure 5.

M. Villegas, T. Jardiel, A.C. Caballero.

Effects of ZnO on the microstructure and electrical properties of WO_3-doped

$Bi_4Ti_3WO_{12}$

Figure 6.

M. Villegas, T. Jardiel, A.C. Caballero.

Effects of ZnO on the microstructure and electrical properties of WO_3-doped
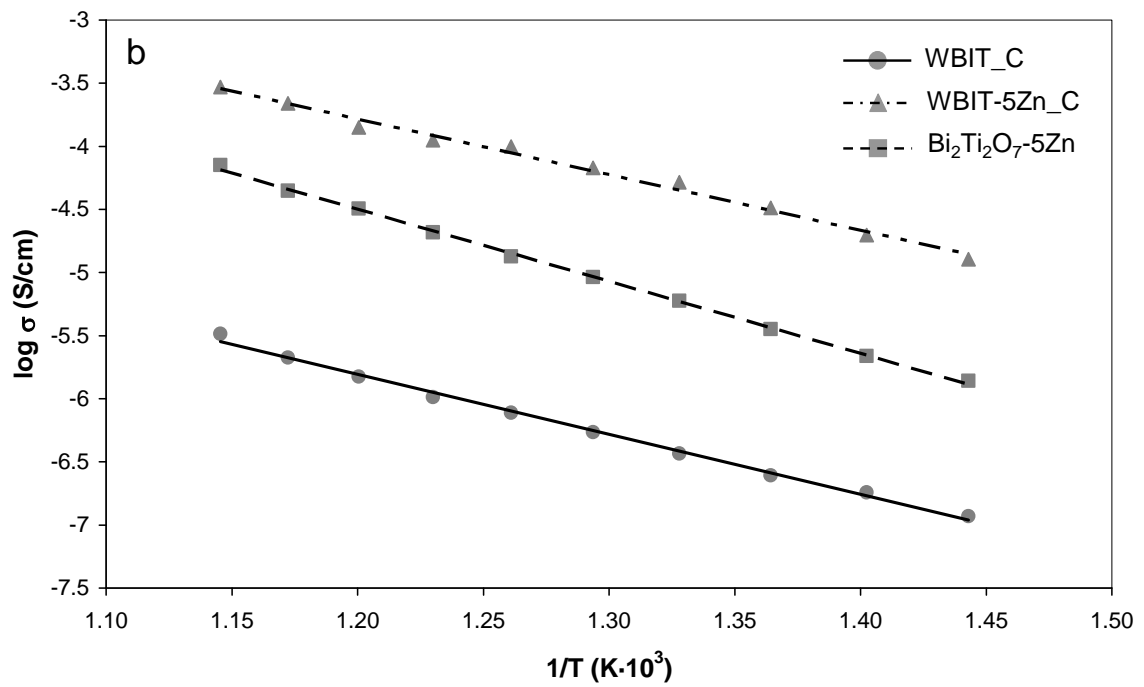
$Bi_4Ti_3WO_{12}$

Figure 7.

M. Villegas, T. Jardiel, A.C. Caballero.

Effects of ZnO on the microstructure and electrical properties of WO_3-doped

$Bi_4Ti_3WO_{12}$

Figure 8.

M. Villegas, T. Jardiel, A.C. Caballero.

Effects of ZnO on the microstructure and electrical properties of WO_3-doped
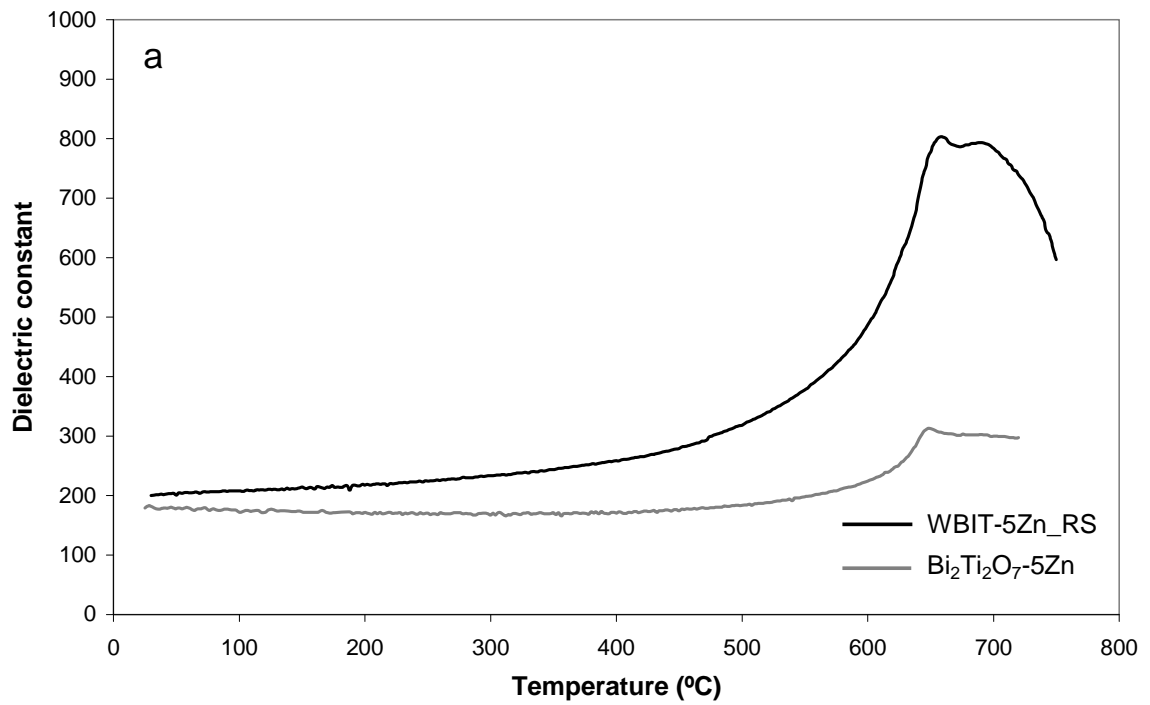
$Bi_4Ti_3WO_{12}$

Figure 9.

M. Villegas, T. Jardiel, A.C. Caballero.

Effects of ZnO on the microstructure and electrical properties of WO_3-doped

$Bi_4Ti_3WO_{12}$